

**ANALYSIS OF  
TRAFFIC FLOW CHARACTERISTICS  
ON SIGNALIZED ARTERIALS**

**Nathan H. Gartner \***

Dept. of Civil and Env'l engineering  
University of Massachusetts  
Lowell, MA 01854, USA

Phone: (978) 934-2289, Fax: (978) 934-3052

email: [nathan\\_gartner@uml.edu](mailto:nathan_gartner@uml.edu)

(written while on sabbatical leave at the  
Institute of Transport Research, German Aerospace Centre)

**Peter Wagner**

Institute of Transport Research, German Aerospace Centre  
Rutherfordstrasse 2, 12489 Berlin, Germany

Phone: +49 30 67055 233, Fax: +49 30 67055 202

email: [peter.wagner@dlr.de](mailto:peter.wagner@dlr.de)

Prepared for presentation and publication  
83<sup>rd</sup> Annual Meeting  
Transportation Research Board  
January 2004  
Washington, D.C.

Revised: December 30, 2003

Text -- No. of Words:	4,100
+6 Figures with Captions:	1,500
<hr/> TOTAL Words:	5,600

*\*Corresponding Author*

**ABSTRACT**

The characteristics of traffic flows on signalized arterials are examined within a cellular automata micro-simulation model. The model is used to analyze arterial throughput and travel times for given densities, coordination schemes and signal spacings. A fundamental 3-D relationship between flow, density and offsets for signalized arterials is established. It is shown, in particular, that arterial throughput is dependent on offsets and that the constituent single intersection limiting capacity, as determined by the saturation flow and the green splits, can only be realized under optimal coordination conditions within a limited range of densities on the arterial. This is a manifestation of the important role that signal coordination and, in fact, Intelligent Transportation Systems (ITS) actions in general play in the operation of urban street networks.

## 1. INTRODUCTION

The use of Cellular Automata in the analysis of traffic systems is becoming increasingly popular in recent years. Cellular Automata (or CA) are mathematical models for complex systems in which many components act together to reproduce complicated patterns of behavior. CA date back to cyberneticist John von Neumann, who in the 1940's wanted to construct a universal Turing machine with the property of self-reproduction (1). CA help to understand the laws that govern complex phenomena by studying the temporal evolution of typical initial conditions under the action of relatively simple local rules. This characteristic is related to synergetics where the cooperation of microscopic simple components produces macroscopic spatial, temporal or functional structures.

Cellular Automata models of traffic, which are based on discretization of time and space, can be considered an alternative and complementary approach to the more traditional models for the representation of traffic flow, such as fluid-dynamic or car-following models (1). In the simplest case, a cellular automaton consists of a line of sites (or, cells) with each site having a value of 0 or 1. The sequence of site values is the configuration evolving in discrete time steps. At each time step the value of each cell is updated according to a given rule. Following are the five fundamental defining characteristics for cellular automata:

1. CA consist of a discrete lattice of sites.
2. CA evolve in discrete time steps.
3. Each site takes on a finite set of possible values.
4. The value of each site evolves according to the same updating rules.
5. Rules for the evolution of a site depend on a local neighborhood of sites around it.

Notwithstanding these simplifications, CA models have found wide applications in the simulation of granular media, fluids, chemical reactions, avalanches and traffic flows. The first traffic implementation of this concept dates back to 1956 when Gerlough developed a simulation model for freeway traffic (3). In the past 20 years there were many applications of CA models to study various traffic flow phenomena (4 - 9). Recently, these models have also been used to study traffic signal operations (10, 11).

In this paper we use a cellular automata micro-simulation model to study traffic flow behavior on a signal-controlled arterial street. A fundamental 3-D relationship between flow, density and offsets, which is commonly used to describe traffic on uninterrupted facilities, is being established here for signalized arterial streets as well. The model is used to analyze arterial throughput and travel times for various densities, coordination schemes and signal spacings. It is shown that arterial throughput is dependent on the offsetting scheme while arterial capacity, as defined by the *Highway Capacity Manual* (12), is not. The arterial capacity is limited by the constituent single intersection capacity as determined by the saturation flow and the green split and is only realized under optimal coordination conditions

for a limited range of densities on the arterial. Section 2 of the paper describes the simulation methodology used to achieve the results which are described in Section 3. The last section summarizes the study findings and draws conclusions.

## 2. THE SIMULATION MODEL

The simulations use the Nagel-Schreckenberg cellular automaton model of traffic flow (5). In this model, a fixed number of cars  $n = 1, 2, \dots, N-1, N$ , with positions  $x_N < x_{N-1} < \dots < x_2 < x_1 \pmod L$ , travel along a loop of length  $L = 3750\text{m}$ . The rules of this model (its car-following dynamics) are defined on a lattice where each cell has a length of  $\lambda = 7.5\text{m}$ , for a total of 500 cells. Time progresses in steps of one second. Since space and time are discrete, so are the speeds of the vehicles. Their speed and position are updated according to the following set of simple rules:

$$\begin{aligned} v_n(t+1) &= \min\{v_n(t)+1, g_n, v_{\max}\} - \xi, \\ x_n(t+1) &= x_n(t) + v_n(t+1) \end{aligned}$$

Where  $g_n = x_{n-1} - x_n - 1$  is the distance to the car in front (front-bumper-to-back-bumper) and  $v_{\max}$  is the maximum speed of the vehicle. In this study all vehicles have the same  $v_{\max} = 3$ , corresponding to 22.5 m/s (50 mph), while  $\xi$  is a random number which is 0 with probability  $1 - p_B$  and 1 with probability  $p_B = 0.1$ .

The behavior of the model can be described as follows: at each time step, the coordinates of each vehicle are updated according to the four rules below. (i) If the speed of a vehicle is lower than  $v_{\max}$ , the speed is increased by 1; (ii) If a vehicle has  $e$  empty spaces in front of it and a speed larger than  $e$ , the speed is reduced to  $e$ ; (iii) The speed of a moving vehicle ( $v_{\max} \geq 1$ ) can be decreased by 1 with braking probability of  $p_B = 0.1$ . This introduces noise to simulate stochastic behavior; (iv) The position of a vehicle is shifted by its speed  $v$ .

In contrast to an open system, where what happens on a link is determined by the interplay between demand and capacity, the system herein is controlled by the global density  $\rho$ . In other words, the fundamental diagram of the system can be described as a function of density only, where the density of the system is set *a priori* and is kept constant for the duration of the simulation run.

The loop  $L$  is divided into segments of equal length  $\delta L$ , each one controlled by a single traffic light at the front end. A preset number of links is designated as traffic lights. Ten traffic lights are used for the analysis, except when studying the effects of signal density, where the number of traffic lights employed is varying between 4 to 20 (corresponding approx. to between 1 and 5 signals/km). The traffic light switches between green and red

periodically. In the green phase vehicles can pass the link, if warranted. In the red phase, vehicles are not allowed to pass and have to wait until the next green. The operation of the traffic light is characterized by the cycle time  $C$  and the green time split  $\alpha = g/C$ . In this study, all traffic lights are operated with the same period  $C = 90s$  and the same  $\alpha = (g/C) = 0.50$ . Furthermore, as the traffic lights are located at equal distances from each other, the same offset  $\phi$  is applied to each. In order to keep things simple, no effects of traffic in the opposite direction, or crossing traffic is considered.

Admittedly, this is a simple model; but, the advantage is that one can focus on important phenomena and analyze them in great clarity without being overwhelmed or distracted by secondary or tertiary effects. Furthermore, even small effects can be properly observed and analyzed. Since all the traffic lights are identical in the present study, results are magnified (by the number of lights) so that we can zoom-in on important phenomena. Although the results are not unique to cellular automata models, they serve as a convenient medium for achieving them. Conventional microscopic simulation models are not geared for this kind of analysis since they are expressly designed for replicating field performance with adequate accuracy. Of course, one can tweak them to perform any programmed task but this is not easy. More realistic simulations can and will be done to assess the myriad of impacts that are being deliberately ignored herein.

As a matter of practicality, the simulation runs in this study were done with 0 to 500 cars on a loop of length  $L=3750m$ , which corresponds to a density range from 0 to 1. The first 2000 time-steps were discarded in order for transients to die down, the next 2000 time-steps were used to acquire results.

### 3. SIMULATION RESULTS

#### 3.1 The Fundamental Diagram

Within this set-up, the fundamental diagram for a signalized arterial has been generated and is shown in Figure 1. The 3D diagram shows the relationship between flow, density and offsets. This can be compared with conventional diagrams for “continuous” or uninterrupted facilities in which flows are typically represented as a function of density and speed. Using the nomenclature of the *Highway Capacity Manual* (12), two principal components make up the total time that a vehicle spends on an arterial: arterial *running time* and *control delay* for the through movement. To calculate the speed we write:

$$ARTSPD = 3,600 * (length) / [(runningtime / km) * (length) + (\sum int .controldelay)]$$

where *ARTSPD* is the arterial *average travel speed* (in km/h). It is a function of the *running time* on the arterial section and the summation of the *control delays* for the through movements at all signalized intersections on the arterial (they are identical in this case). To calculate the flow on the arterial we can write:

$$ARTFLOW = ARTSPD * DENSITY$$

This shows that for a given density the *arterial flow rate* (or *throughput*) is inversely dependent on the intersection *control delay*. Since the latter is a function of the coordination scheme (or, offsetting) we obtain the fundamental diagram for a signalized arterial where the commonly used speed axis is supplanted by the offset axis. We have deliberately chosen to employ here the term throughput rather than volume, although the two terms are being used interchangeably in some cases. There is a subtle but important distinction that is pertinent in this context: *Throughput* is an active term describing the output from a facility which is dependent on the way it is being operated or controlled. On the other hand, *volume* is a more passive term commonly used to describe the demand for travel on the facility irrespective of the way it is operated. Thus *capacity* flow on the facility is attained only when the maximum value of throughput can be realized. The distinction is further elaborated in Section 3.2.

The different regions in the diagram can be analyzed in a similar way to those on uninterrupted facilities as described below.

### *Uncongested Regime*

When density is *low* and there is no congestion, the stochasticity of the model does not matter much and one gets, as expected, the maximum in traffic flow when the offset time is set to the expected travel time on each signalized link:

$$\phi = \delta L / \langle v \rangle = \delta L / (v_{\max} - p_B).$$

At this setting delay is minimized, speed is maximized and, for a given density, flow is also maximized. Since the maximal flow rate is periodic with the offsets, we can write:

$$\phi + kC = \delta L / \langle v \rangle \quad \text{where } k \text{ is an integer.}$$

Figure 2 portrays a 2D projection of the 3D data in Figure 1, depicting the familiar flow vs. density coordinates. Shown (in red dots) are the variations in flow caused by different offsets at specific density values. The curve for random offsets (blue line) is shown to be at an intermediate level between “good” and “poor” progressions. Since the flow is the product of speed and density  $q = v \cdot \rho$ , then for any specific density it is proportional to the speed which, in turn, depends on the offsets. An improved progression increases speed and, with it, the throughput. This is the essential role of coordination on arterial streets.

### *Saturation: At the Brink*

When density increases to an *intermediate* value, traffic flow is observed to saturate to a constant maximum value, which (in this case) is equal to a fixed fraction  $\alpha = 0.50$  of the maximum flow if there were no traffic lights. This can be seen in Fig. 2 where the

highlighted (blue) curve with random offsets has about  $\frac{1}{2}$  the height of the curve (in purple) with no signals. Thus, in the intermediate density region, while traffic flow is at a maximum, vehicles are caught in stop-and-go cycles due to un-dissolved queues from downstream signals. Offset variations have little effect on throughput in these circumstances and we see that the (red) dot spread is reduced to a sliver.

### *Congested Flow*

In the *high-density* region, when traffic jams become dominant, the downstream green has to start ahead of the upstream green in order to clear the accumulated traffic on each link. The optimal offsets are then negative and we get the well-known phenomenon of “reverse progressions” (13).

The variation of flow with offsets can be seen more dramatically in Figure 3, which presents two cuts through the 3D surface of Figure 1: one at a low density  $\rho = 0.10$  and the second at a high density of  $\rho = 0.86$ . For the low-density curve (red line), the parameters that are used are:  $\delta L = 375\text{m}$ ,  $v_{\max} = 3$  (22.5 m/s) and  $p_B = 0.1$ ; therefore, optimal progression should be at  $\phi = \delta L / \langle v \rangle = \delta L / (v_{\max} - p_B) = 17.24\text{s}$ . Indeed, as shown in the graph, the maximum flow is located at  $\phi = 18\text{s}$  in this case. The cycle time is fixed at  $C = 90\text{s}$ . As expected, at low density there is almost a 1:4 ratio between the low point of flows (poor offsets) and the high point (optimal offsets). The respective flows are  $q = 0.07\text{vps}$  (250 vph) vs.  $q = 0.275\text{vps}$  (990 vph). One has to remember that the results are magnified by the fact that there are 10 traffic lights on the ring. The effect attributable to any one light is only  $1/10^{\text{th}}$  of the total.

If one would plot average delay per vehicle as a function of offset, one would obtain a function that is the mirror image (i.e., an inverted image) of the red curve. This is the more familiar offset-delay function, such as the one that was experimentally validated in a study that was conducted at the Toronto Traffic Control Centre by Gartner (14). Such functions have also been used in various signal optimization procedures, e.g., SIGOP and MITROP (15). Using such functions one can verify that when offsets are close to optimality we have lower delay, higher travel speed and, consequently, a higher flow rate.

For the high density curve (green line), the “backward progression” can be seen to occur at about  $\phi = -50\text{s}$ . The respective values for the flows in this case are  $q = 0.075\text{vps}$  (270 vph) vs  $q = 0.115\text{ vps}$  (414 vph) for a ratio of 1:1.5 which is much lower than in the low density case. Again, the contribution of any single signal is only  $1/10^{\text{th}}$  of the total. i.e., a 5% increase per signal. Such a small effect might not be observable in conventional microscopic simulation models where the multitude of stochastic phenomena would muffle it. Clearly, coordination effects are more pronounced in low-density (free-flow) conditions than in high-density (congested) conditions.

Fig. 4 illustrates the relationship between flow and travel time. The upper (red) graph is for an uninterrupted arterial (no traffic signals), the bottom (green) is for the signalized arterial with random offsets. The same phenomena are demonstrated. In the uncongested region,

travel time ( $tt$ ) is almost independent of flow, which is due to the fact that vehicles can move with maximum speed. In the congested region, which corresponds to large densities, travel time increases rapidly and there exists almost a proportional relationship between flow and the inverse of the travel time, i.e.,  $q \propto 1/tt$ .

### 3.2 Throughput and Capacity

Considering the data in Figures 1-4, the question arises, naturally, do offsets affect capacity? Strictly speaking, and using the definition of the *HCM* (12) which says that “the capacity of a facility is defined as the *maximum* hourly rate at which persons or vehicles can reasonably be expected to traverse a point or uniform section of a lane or roadway during a given time period under prevailing roadway, traffic, and control conditions,” then offsets have virtually no effect on capacity. Figure 2 shows that the capacity of the facility that is analyzed herein is  $c = 0.29\text{vps}$  (1045 vph). This is one-half the value of the capacity that would be obtained on this facility if it had no signals and the flow would be uninterrupted  $q_s = 0.58\text{vps}$  (2090 vph). This follows from the relationship  $c = \alpha q_s$ , where  $q_s$  is the saturation flow, i.e., the flow that can be realized when the signal indications are continuously green ( $s$  is used for this variable in the *HCM*).

It is seen that capacity flows can be attained within a range of densities; however, there is only one density, call it  $\rho_m$ , at which capacity is independent of offsets. In the case studied herein this density is  $\rho_m = 0.39$ . At this point, varying the offsets has no effect on flow. In contrast, at both the lower density region and the upper density region offsets have considerable effect on flows and, thus, on throughput. Therefore, we can say that offsets have a significant impact on the throughput of a signalized arterial but not on its (inherent) capacity. This is illustrated by the red dots in Fig. 2. Capacity flow (i.e., the maximum possible flow rate) is attained at  $\rho_m$  and when optimal offsets are in effect within a range of other densities. At some densities in the very low and very high ranges capacity flow can not be attained. In the first case, because there is not enough demand; in the second, because the demand cannot move with sufficient speed.

Some authors have argued that capacity is different under “favorable” and “unfavorable” progression (16). Those results were calculated by using a microscopic simulation model. While the numerical results are correct, their interpretation is not. What has been shown in these studies is that a higher *throughput* can be obtained under favorable progression. The “capacity” of the facility stays the same irrespective of the progression. Each of the simulation results considers only one coordination scheme, i.e., one operating point (or dot in our scheme). By using cellular automata simulation one can obtain a comprehensive view, which encompasses the entire range of parameters, as illustrated by the 3D diagram in Fig. 1. Furthermore, by using a ring road with 10 traffic lights in one direction, effects of (good or bad) coordination are amplified so that their effect is more pronounced.



A simple and obvious conclusion from the discussion above is that one should always strive to obtain an optimal coordination. This does not only reduce delay and increase speed (i.e., reduce travel time) but, more importantly, helps to increase throughput. Unfortunately, in practice, this is not always possible. Here are some of the reasons:

1. Arterial progressions must be compromised on two-way streets since the offsets are common to both directions; schemes in which one direction is favored during certain times are often used.
2. Offset determination is constrained in grid networks due to the notorious “loop constraints” (17). Priority routes may be created on which preferential offsets are established.
3. Traffic-adaptive schemes may sacrifice arterial coordination benefits in favor of local responsiveness. The trade-offs must be carefully evaluated in this case: local advantages may compromise global throughput.

### 3.2 Effects of Signal Density

Travel characteristics on signalized arterials are significantly affected by the frequency at which traffic lights are encountered, i.e., the signal spacing. This can easily be investigated in the CA model by varying the section length  $\delta L$ . For a given (fixed) density, the 3D diagram illustrating flow as a function of offsets and signal spacing is shown in Fig. 5. The number of traffic signals on the loop is varied between 4 to 20 (corresponding, approx., to between 1 and 5 signals/km). A wave-like surface is obtained with respect to the offset. The period is, again, 90s due to the fixed cycle length of the same magnitude. Since all cars in the simulation have the same maximum speed, almost no platoon dispersion is observed. Therefore, the maximum flow that can be achieved (i.e., the *capacity*) does not decline as a function of the distance between the traffic signals. What declines, however, is the discrepancy between the worst possible and the best possible choice of offset  $\phi$ .

Figure 6 is a 2D condensation of the data in Fig. 5 for a fixed (low) density. The upper (blue) line indicates the best possible offset and the lower (red) line the worst. The discrepancy increases with signal density since signal delay becomes a larger proportion of the total travel time when there are more signals on the same road length.

#### 4. CONCLUSIONS

Cellular automata models have gained popularity in recent years, though their application in traffic simulations dates back half a century. This study shows that these models can be used to demonstrate important traffic flow characteristics in a clear and convincing way.

A simple cellular automata (CA) model is being used to investigate characteristics of traffic flow on signalized arterials and to contrast them with those for uninterrupted highway facilities. A fundamental diagram for signal-controlled arterials (in 3D) relating flow to density and offsets is generated. It is shown that, for a given density, throughput is strongly correlated with offsets (for any given cycle time and green splits), since offsets determine the progression speed. On the other hand, arterial capacity, using the definition of the *Highway Capacity Manual* in the strictest sense, is not affected by coordination.

Arterial progression is commonly related to travel times, travel speeds, delays and level-of-service. In this study it is clearly shown that it ought also to be related to throughput. This is not well recognized in the literature or in practice. In a broader sense, this is the goal of most ITS actions: the reduction of travel time and increase of average speed which, in turn, increase throughput or overall productivity of the transportation system.

#### REFERENCES

1. Gartner, N. H., C.J. Messer and A.J. Rathi. *Traffic Flow Theory: A State-of-the-Art Report*. FHWA Fairbanks Highway Research Center, McLean, VA. URL: <http://www.tfhr.gov/its/tft/tft.htm>, 1996.
2. von Neumann, J. *Theory of Self-Reproducing Automata* (Ed.: A.W. Burks). University of Illinois Press, Urbana, 1966.
3. Gerlough, D. L. *Simulation of Freeway Traffic by an Electronic Computer*. Procs., 35<sup>th</sup> Annual Meeting of the Highway Research Board, Washington, D.C., 1956.
4. Cremer, M. and J. Ludwig. *A fast simulation model for traffic flow on the basis of Boolean operations*. Mathematics and Computers in Simulation, 1986.
5. K. Nagel and M. Schreckenberg. *A cellular automaton model for freeway traffic*. J. Physique I, 2221, 2, 1992.
6. Daganzo C.F. *The Cell transmission model: a simple dynamical representation of highway traffic*. Transportation Research B 28, 269 – 287, 1994.

7. Krauss S., K. Nagel and P. Wagner. *The mechanism of flow breakdown in traffic flow models*. Compendium of papers presented at the 14<sup>th</sup> Intern. Symp. on Transportation and Traffic Theory (A. Ceder, Editor). Jerusalem, Israel, July 1999.
8. Chowdhury D., L. Santen, and A. Schadschneider. *Statistical Physics of Vehicular Traffic and Some Related Systems*, Physics Reports **329**, 2000. [See also at [arxiv.org/abs/cond-mat/0070053](http://arxiv.org/abs/cond-mat/0070053)].
9. Helbing D. *Traffic and Related Self-Driven Many-Particle Systems*, Reviews of Modern Physics **73**(4), 1067-1141, 2001. [See also at [arxiv.org/abs/cond-mat/0012229](http://arxiv.org/abs/cond-mat/0012229)]
10. Huang D.-W. and W.-H. Huang. *Traffic signal synchronization*, Phys. Rev. E **67**, 2003.
11. Brockfeld E., R. Barlovic, A. Schadschneider, and M. Schreckenberg. *Optimizing Traffic Lights in a Cellular Automaton Model for City Traffic*. Phys. Rev. E **64**, 2001.
12. *Highway Capacity Manual 2000*. Transportation Research Board, Washington, DC , 2000.
13. Lieberman E.B., J. Chang and E.S. Prassas. Formulation of real-time control policy for oversaturated arterials. Transp. Res. Record 1727. TRB, 2000.
14. GARTNER N. Microscopic Analysis of Traffic Flow Patterns for Minimizing Delay on Signal-Controlled Links. Highway Research Record 445. HRB, pp. 12-23, 1973.
15. *Traffic Control Systems Handbook*. Report No. FHWA-SA-95-032. Federal Highway Administration. U.S. Dept. of Transportation, Washington, DC, 1996.
16. Olszewski P. Comparison of the HCM and Singapore Models of Arterial Capacity. Procs., TRB Highway Capacity Committee Summer Meeting (W. Brilon, Editor), Hawaii, 2000.
17. Gartner N. H. and Ch. Stamatiadis. Concurrent Progression Schemes in Multi-Arterial Traffic Networks Using MULTIBAND. Procs., 68<sup>th</sup> Annual Meeting of the Institute of Transportation Engineers. Toronto, Ontario, August 1998.

## LIST OF FIGURES

Figure 1. The fundamental diagram as function of offset  $\phi$  and density  $\rho$ .

Figure 2. The fundamental diagram as function of density only. A comparison between a random offset strategy (blue) and the fundamental diagram of the system without traffic lights (purple). The red dots are simulation results for various offsets.

Figure 3. Plotted is the flow  $q = \langle v \rangle \rho = \sum_{i=1}^N v_i / L$  of the road (averaged over the whole system) as function of offset  $\phi$ , for a low density ( $\rho = 0.1$ ) and a high density case ( $\rho = 0.86$ ). The parameters used are  $\delta L = 375m$ ,  $v_{\max} = 3$  (22.5m/s) and  $p_B = 0.1$ , therefore optimal progression should be at  $\phi = \delta L / \langle v \rangle = \delta L / (v_{\max} - p_B) = 17.24s$ . Indeed, the maximum of the flow is located at  $\phi = 18$ . The cycle time is fixed at  $C = 90s$ . For the large density, the backward progression can be seen to occur around  $\phi = -52$ .

Figure 4. Flow as function of travel time. The upper (red) graph is for an uninterrupted arterial (no traffic lights), the bottom (green) for the signalized arterial with random offsets.

Figure 5. Flow as function of traffic signal density and offset  $\phi$ . Due to the fact that all cars in the simulation have the same maximum speed, almost no platoon dispersion is observed. Therefore, the maximum flow achievable does not decline as a function of distance between the traffic lights. What declines, however, is the difference between the worst possible and the best possible choice of offset  $\phi$ .

Figure 6: Two-dimensional condensation of the data in Fig. 5 for a fixed (low) density. The upper (blue) line indicates the best possible offset and the lower (red) line the poorest. The difference increases with signal density as signal delay becomes a larger proportion of total travel time.

FIGURE 1

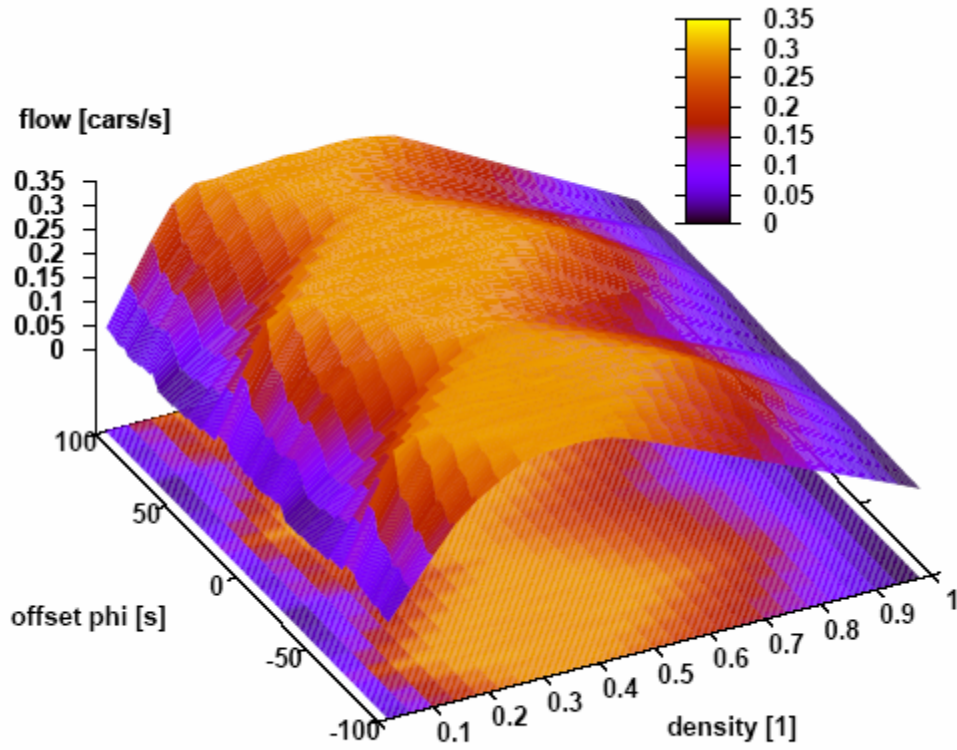


FIGURE 2

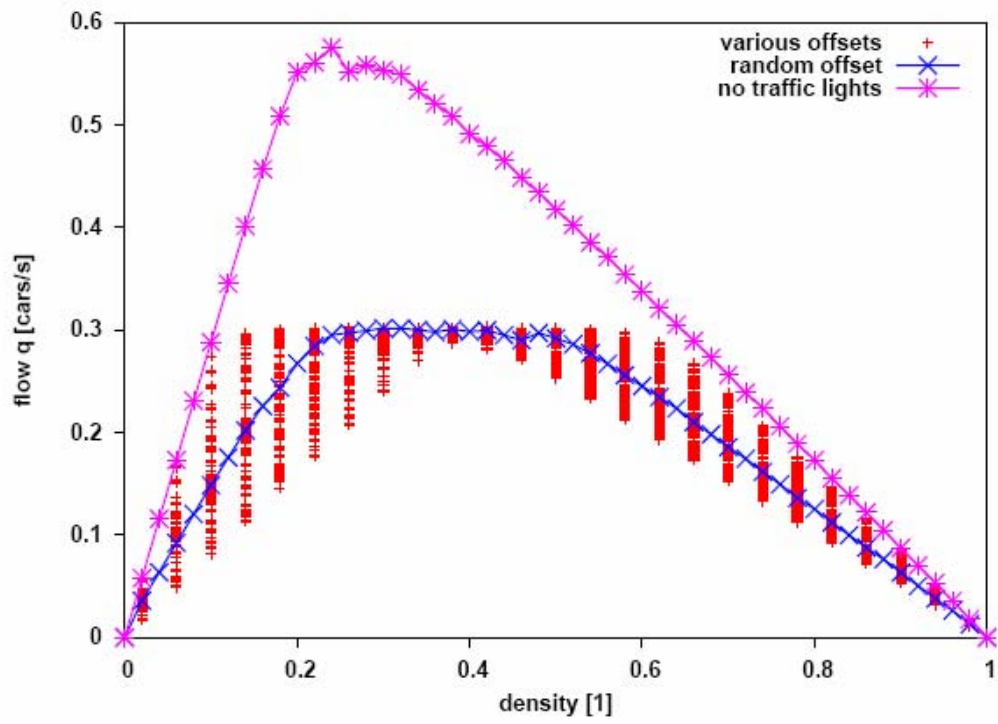


FIGURE 3

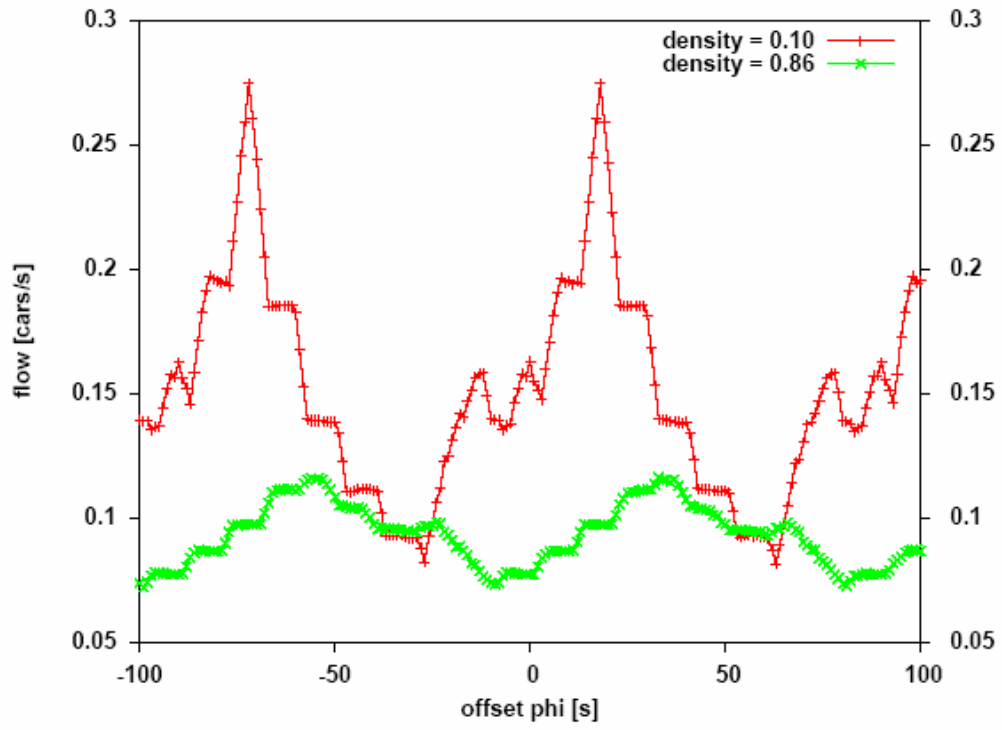


FIGURE 4

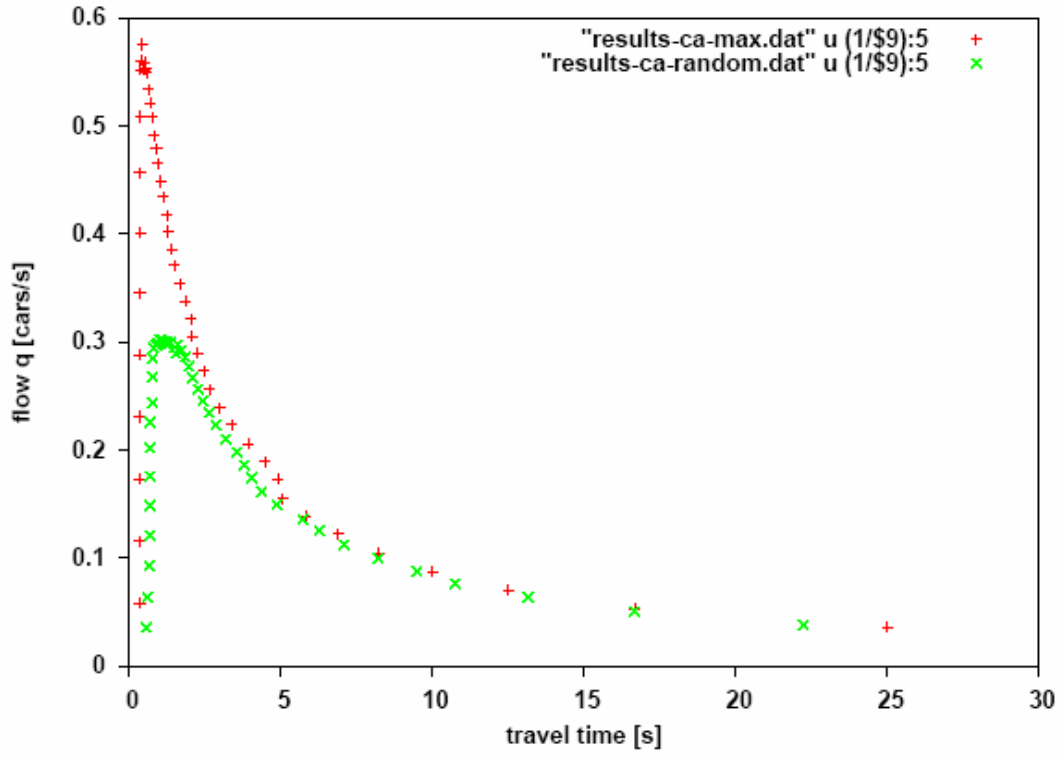




FIGURE 5

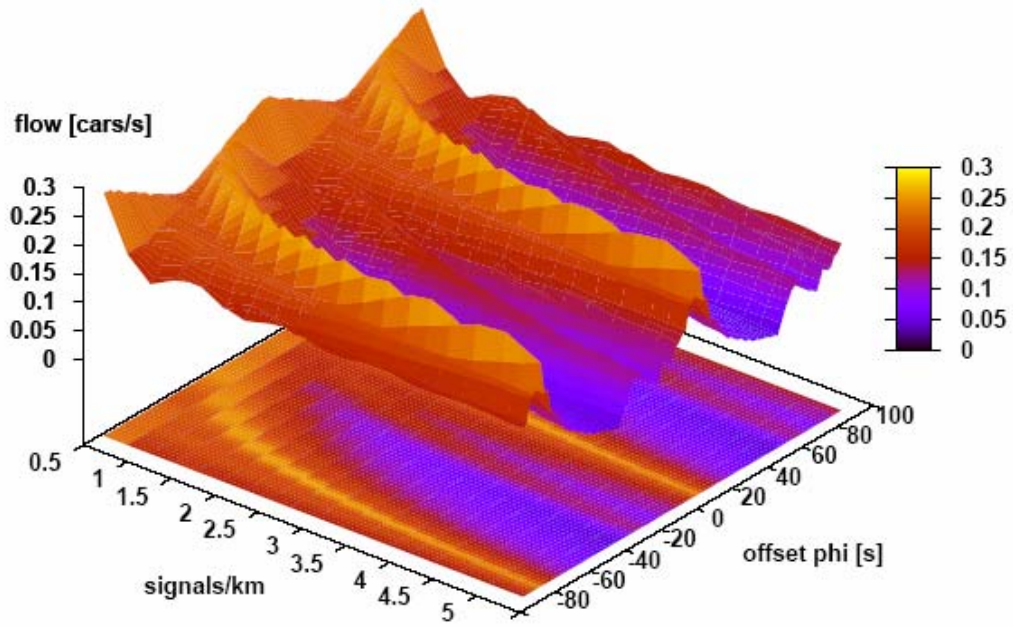


FIGURE 6

